Determination of time-domain migration velocities from CRS attributes

José Silas dos Santos Silva*[1] and German Garabito[1,2], [1]PPGCEP/UFRN, [2]DPET/CT/UFRN

Abstract

The kinematic wavefield attributes of the common-reflection-surface (CRS) stack method have several applications for solving important seismic reflection imaging problems. These kinematic attributes, also called CRS attributes, are extracted from the multi-coverage prestack data using multidimensional global optimization algorithms. Commonly, these attributes are successfully applied to determine the depth-domain velocity model by mean of tomography, however, there is still no practical and efficient algorithm to determine the migration velocity model in the time domain. We present an algorithm to semi-automatically determine the migration velocity in the time domain from the CRS attributes picked along the main horizons in the zero-offset CRS stacked section. We explain the main steps of the proposed algorithm by applying it to synthetic data and we demonstrate that the obtained velocity model is accurate and useful for application in the time migration.

Introduction

The CRS stack method was introduced to simulate zero-offset (ZO) stacked data from multi-coverage reflection seismic data (Müller et al., 1988; Jäger et al., 2001). This method does not require explicit knowledge of the velocity model and determines the kinematic wavefield attributes, also called CRS attributes, from the pre-stack data to define the stacking operator and simulates the ZO stacked data. In 2D, the data-driven CRS stack method depends on three kinematic wavefield attributes, namely, the wavefronts of the normal-incidence-point (NIP) wave and the Normal wave, and the emergence angle of the ZO central ray, all of them emerging at the acquisition surface.

The CRS attributes are extracted from prestack multi-coverage reflection data by means of optimization strategies based on seismic coherence measurement of the seismic signal. Jäger et al. (2001), Mann (2001) and Garabito et al., (2001) introduced multi-step strategies to determine the CRS attributes, that is, they are searched separately in the common-midpoint (CMP) gathers, in the ZO stacked section and also using a set of gathers. To prevent the propagation of attribute errors in the various steps, Garabito et al. (2012a) proposed the simultaneous determination of the three attributes by means of global optimization from subsets of prestack multi-coverage data, thus estimating more accurate attributes for applications in seismic reflection problems.

These three kinematic wavefield attributes, the CRS stacking operator and its particular case the common diffraction (CDS) stacking operator have several applications in seismic reflection problems, such as, velocity model determination in depth domain through tomography (Duveneck, 2004), prestack migration depth and time migrations (Spinner and Mann, 2007; Garabito et al., 2012b; Garabito, 2018), prestack data interpolation and enhancement (Baykulov and Gajewski, 2009; Garabito, 2021).

Currently, the main application of the CRS stack method is for interpolation and enhancement of prestack seismic data from onshore basins. Therefore, CRS-based reconstructed data can be used for prestack-time-migration (Gierse et al., 2008; Garabito et al., 2015) and for prestack-depth-migration (Schuenemann et al., 2011; Gierse et al., 2015; Garabito et al., 2020). The same reconstructed data can be used for depth velocity model building, for standard time domain velocity analysis based on normal moveout (NMO) correction and for residual migration velocity analysis.

A few works introduced approaches to apply the CRS attributes directly to determine the time migration velocity model. For instance, Garabito et al. (2011) generated synthetic diffractions using the NIP-wave attributes and CDS stacking operator, and the migration velocities are picked by means of interactive diffraction focusing analysis. Glöckner et al. (2019) presented an approach to calculate automatically the time-domain migration velocity model from the kinematic CRS attributes using an equation that relates the CRS attributes to the migration velocities. In this approach, the estimated velocities could present anomalous values related to the coherent noise present in the data. The gaps produced by a coherence filter are filled using an interpolation method based on a least-squares approach, afterwards a smoothing filter is applied to obtain the migration velocity model.

However, there is still no well-established practical algorithm to determine the time migration velocity model developed using the CRS stack method. In this work, we present a practical algorithm to build the migration velocity model in time domain from the CRS attributes. We start by simultaneously researching the three CRS attributes using global optimization, and then they are smoothed out to correct anomalous fluctuations due to the optimization process. To avoid wrong velocity values due to coherent noise present in the data or other false events, we apply picking of the main horizons to extract the CRS attribute and automatically calculate migration velocities. We validate the proposed algorithm using multi-coverage synthetic seismic data of a model with smoothly folded homogeneous layers.

CRS stacking operator and wavefield attributes

The CRS stack method uses a second-order traveltime expansion derived from paraxial ray theory (Schleicher et al., 1993), which depends on three parameters or kinematic wavefield attributes. This hyperbolic traveltime approximates the reflection times of rays with arbitrary half-offsets (*h*) and midpoints (*m*) close to the vicinity of a ZO central ray (Tygel et al., 1997)

$$t^2(\Delta m, h) = (t_0 + p\,\Delta m)^2 + q(K_N \Delta m^2 + K_{NIP} h^2), \quad (1)$$

with

$$p = \frac{2\,sin\,sin\,\beta_o}{v_0} \quad and \quad q = \frac{2t_0\,cos\,cos\,\beta_0}{v_0}$$

The midpoint displacement between the paraxial ray and central ray is denoted by $\Delta m = m - m_0$, the quantity t_0 is the two-way reflection traveltime of the ZO central ray and v_0 is the constant near surface velocity. The three-unknown kinematic wavefield attributes are the emergence angle (β_o) of the central ray and the two wavefront curvatures (K_N, K_{NIP}) that correspond to the emerging hypothetical normal and NIP waves as defined by Hubral (1983).

Considering that the three kinematic attributes for a given ZO sample point on a reflection event are known, the traveltime equation (1) defines a stacking surface, also called CRS stacking operator, in the midpoint and half-offset space. In the CRS stack method, the seismic amplitudes of the prestack data are summed along the CRS stacking operator to obtain a ZO staked amplitude. The repetition of this stacking process for all samples of the ZO section to be simulated produces the CRS ZO stacked section.

A special case of equation (1) can be obtained when the wavefront curvature of the normal wave is equal to the wavefront curvature of the NIP wave, i.e., $K_N = K_{NIP}$. This means that the reflector element collapses in a diffractor, and as result we obtain the common-diffraction-surface (CDS) stacking operator, which depends only on two attributes (β_0, K_{NIP}) called here as NIP wave attributes. The CDS stacking operator approximates the standard Kirchhoff prestack time migration operator in the midpoint and half-offset space. So, considering $h = 0$ and applying the diffraction condition $K_N = K_{NIP}$ in equation (1), we obtain the CDS operator for ZO geometry

$$t^2(\Delta m) = (t_0 + p\,\Delta m)^2 + q\,K_{NIP} \Delta m^2, \quad (2)$$

CDS operator (2) is referenced to the stationary point at (m_0, t_0) and also approximates the Kirchhoff post-stack time migration operator. To apply equation (2) for post-stack time migration that places the stacked amplitudes along the hyperbole at its apex, we need to obtain the analytical expressions of the apex location (x_{ap}, t_{ap}) of the equation (2) by applying the derivative in relation to the midpoint *m* and equaling it to zero, so the result is (Mann 2002)

$$x_{ap} = x_0 - \frac{t_0 v_0 R_{NIP}\,sin\,sin\,\beta_0}{t_0 v_0\,\beta_0\; + 2R_{NIP}\,\beta_0}, \quad (3a)$$

$$t_{ap}^2 = \frac{t_0^3 v_0 \beta_0}{t_0 v_0\,\beta_0\; + 2R_{NIP}\,\beta_0}. \quad (3b)$$

Expressing equation (2) in terms of apex coordinates of equation (3), we obtain the CRS-based hyperbola equation for post-stack time migration expressed in terms of apex (x_{ap}, t_{ap}) and by analogy we also obtain the migration velocity expressed in term of NIP wave attributes (Mann, 2002)

$$v_{ap}^2 = \frac{2v_0^2 R_{NIP}}{t_0 v_0\,\beta_0\; + 2R_{NIP}\,\beta_0}, \quad (4)$$

Using equation (4), we can automatically calculate the migration velocity that is referenced to the apex of the CDS operator (2).

On the other hand, the CDS operator and the NIP wave attributes have several applications in reflection seismic imaging. In this work, as in Garabito et al. (2011), we will also apply the CDS operator (2) and the NIP wave attributes to generate synthetic diffractions on the ZO CRS stacked section by applying the demigration operation. These synthetic diffractions will be used for quality control of the migration velocity calculated using the algorithm proposed below.

Algorithm to calculate the migration velocity

Despite the possibility of automatically calculating the migration speed with equation (4), it is necessary to establish restrictions to avoid errors due to the CRS attributes being associated with different types of noise. An important constraint to avoid anomalous values is to calculate velocities only for the most important reflection events or seismic horizons. On the other hand, to correct the non-physical fluctuations in the values of the CRS attributes, a smoothing filter must also be applied after being estimated by optimization. Taking these considerations into account, we propose the following algorithm to calculate the migration velocities from the CRS attributes:

1) Application of the CRS stack method to obtain the tree kinematic wavefield attributes and the ZO stacked section.
2) Smart smoothing of the kinematic wavefield attributes.
3) Semi-automatic picking of the main seismic horizons in the CRS ZO stacked section.
4) Calculation of the migration velocities using the equation (4) for the picked attributes.
5) Interpolation of the velocities in the time axis and after in the midpoint axis.

The output of this algorithm is the time-domain migration velocity model suitable for prestack or post-stack time migration.

To perform the semi-automatic picking of the CRS attributes of the main reflection events or horizons in the CRS ZO stacked section, we use the algorithm proposed in Gadelha et al. (2009), where the local slope, calculated from the emergence angle of the ZO central ray and the near surface velocity, is used to track a reflection event and automatically pick points on the reflections. The picking process of a reflection event starts with a manual pick of a point and for this reason is called semi-automatic picking algorithm

Numerical results

In order to validate the algorithm proposed before, we use a synthetic model composed of smoothly folded homogeneous layers shown in Figure 1. This model presents lateral variation of the near-surface velocity, that is, it has 1800 m/s on both sides and 2200 m/s in the center of the model. We generate multi-coverage synthetic seismic data using a finite difference solution of the acoustic wave. The dataset has 251 shots with an interval of 40 m between shots and 126 traces each, and with an interval of 20 m between consecutive traces. The minimum offset is 0 m and the maximum absolute offset is 2500 m. The time sample interval is 4 ms and the maximum trace length is 2.5 s.

The synthetic seismic data of this model will allow us to evaluate the sensitivity of the near-surface velocity in the determination of the CRS attributes and, particularly, in the determination of the migration velocities. In this study, to perform the CRS stacking and simultaneously determine the three CRS attributes, we use the one-step global optimization strategy presented in Garabito et al. (2012a). We only show the CRS ZO stacked section in Figure 2, but the three kinematic wavefield attributes that are used to calculate velocities are not shown.

As the data is synthetic and has no noise, the CRS attributes do not have fluctuations and outliers, therefore, it was not necessary to apply the smoothing filter. We apply the semi-automatic picking algorithm to extract the NIP wave attributes along the reflection events, and the result is shown in Figure 2 as red dots over the reflection events.

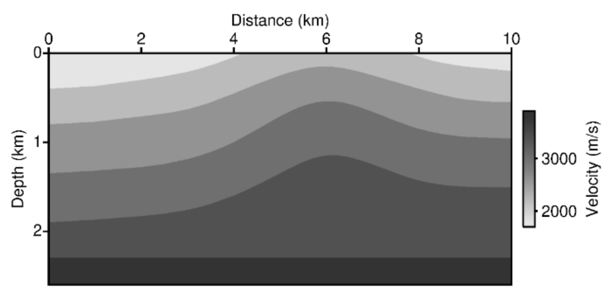

Figure 1 – Synthetic velocity model composed of smoothly folded homogeneous layers.

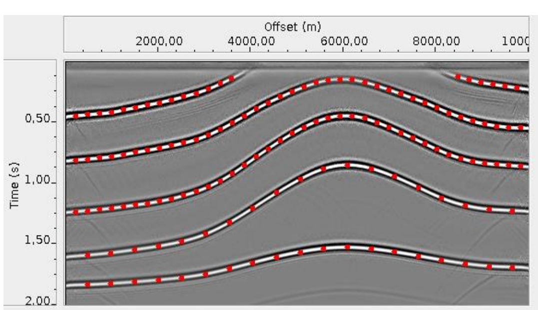

Figure 2 – CRS ZO stacked section simulated from the synthetic data of the model shown in Figure 1. The red dots are the results of the semi-automatic picking.

From the picked points for each horizon, we calculated the apex of the hyperbola or CDS operator using the equation (3), and the results are shown with blue lines in Figure 3a. In the same figure, we show the reflection traveltimes that are also related to the picked red points shown in Figure 2. We can see that both curves are coincident in places where the reflections are close to the horizontal and, as expected, they diverge in places where the reflections have steep dips.

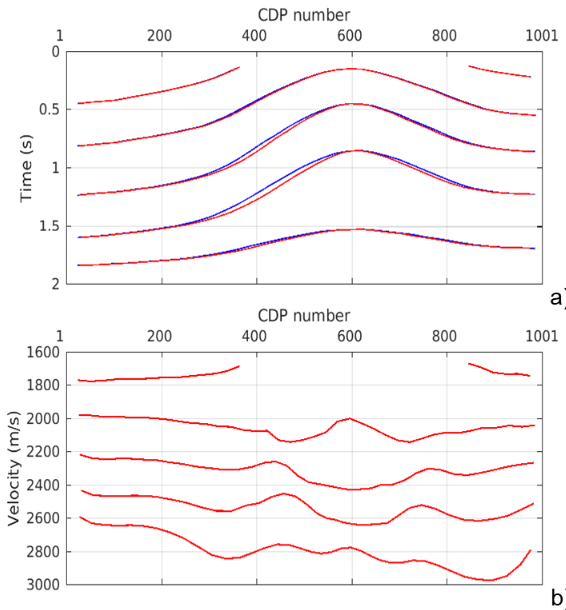

Figure 3 – Results related to the picked points of Figure 2: a) reflection traveltimes (blue lines) and CDS operator apex positions for each picked point (red lines), b) migration velocities calculated for each picked point on the horizons.

According to step 4 of the proposed algorithm, from the NIP wave attributes extracted for the picked points, we calculate the migration velocities using equation (4) and the result is shown in Figure 3b, where the red lines are the velocities for each horizon. Following the algorithm, from the results shown in Figure 3b, we apply an interpolation of the velocities first on the time axis for each CMP location and also after the interpolation is performed on the CMP coordinate. Figure 5a shows the migration speed model obtained from the CRS attributes and without any smoothing and editing. For comparison, we show in Figure 5b the time-domain root-mean-square (RMS) velocity model calculated from the velocity model in Figure 1.

To assess the accuracy of the velocity model obtained by the proposed approach, we applied the Kirchhoff post-stack time migration (PostSTM) to the CRS ZO stacked section shown in Figure 2. Before applying the migration, to have a migration quality control parameter, for each picked point in the ZO section we generate synthetic diffractions using the CDS operator (2) and the demigration process. Figure 5a shows the migrated image with the velocity model of Figure 4a and Figure 5b is the migrated image obtained with the velocity model of Figure 4b. We note that the migration velocity calculated from the CRS attributes produces a more accurate migrated image, with the synthetic diffractions well collapsed. As expected, the RMS speed model provides a migrated image with poorly collapsed diffraction events, because this velocity does not take the dipping effect into account.

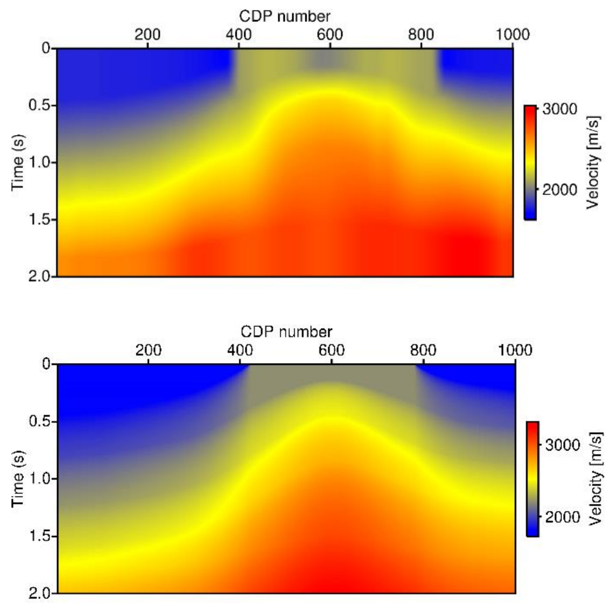

Figure 4 – Velocity models in time domain obtained for the synthetic model shown in Figure 1: a) Migration velocity model obtained from the CRS attributes and b) RMS velocity model calculated from the true velocity model in Figure 1.

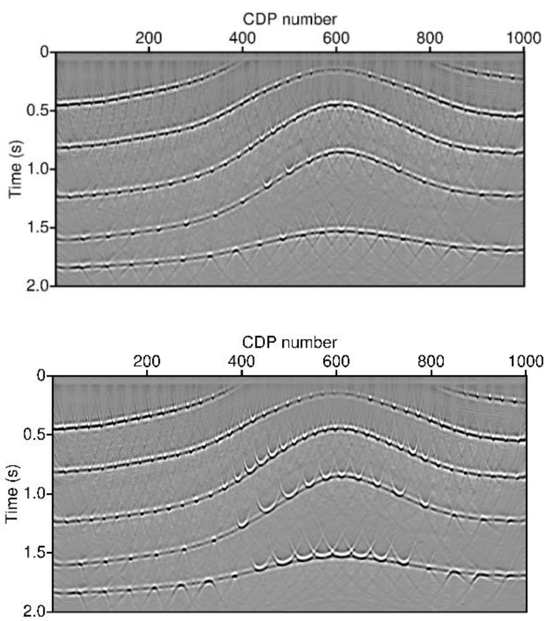

Figure 5 – Kirchhoff PostSTM images obtained from the CRS ZO stacked section with added synthetic diffractions using: a) migration velocity model shown in Figure 4a and b) RMS velocity model shown in Figure 4b.

Conclusions

We present a practical and efficient algorithm to build the time-domain migration velocity model from the CRS attributes. We demonstrate its accuracy and applicability in synthetic seismic data from a heterogeneous model composed of layers that form a smooth anticline fold.

The PostSTM image with well-collapsed synthetic diffractions demonstrates that the migration velocities obtained from the CRS attributes have good precision, even when the medium has variable velocities close to the surface. This example demonstrates that the proposed algorithm can be applied to real data where the velocity near the surface is variable.

For application in real data of structurally complex geological media, it will be necessary to include in the algorithm an interactive quality control step, which can be implemented with the help of synthetic diffractions.

Acknowledgments

The first author thanks CAPES for granting the master's scholarship.

References

Baykulov, M., and D. Gajewski, 2009, Prestack seismic data enhancement with partial common reflection surface (CRS) stack: Geophysics, 74, no. 3, V49–V58.

Duveneck, E., 2004, Velocity model estimation with data-derived wavefront attributes:Geophysics 69, 265–274.

Gadelha, I., Lima, A. W., and Garabito, G., 2009, Picking interativo dos atributos CRS e tomografia da onda NIP: Aplicação em dados da Bacia do Tacutu: 11th International Congress of SBGf, Expanded Abstracts.

Garabito, G., P. L. Stoffa, L. S. Lucena, and J. C. R. Cruz, 2012a, Part 1 - CRS stack: Global optimization of the 2D CRS-attributes: Journal of Applied Geophysics, 85, 102–110.

Garabito, G., P. L. Stoffa, C. S. Ferreira, and J. C. R. Cruz, 2012b, Part II - CRS-beam PSDM: Kirchhoff-beam prestack depth migration using the CRS stacking operator: Journal of Applied Geophysics, 85, 92–101.

Garabito, G., 2018, A comparative study of common-reflection surface prestack time migration and data regularization: Application in crooked-line data: Geophysics, 83, no. 4, S355–S364.

Garabito, G.,2021, Prestack seismic data interpolation and enhancement with common-reflection-surface-based migration and demigration. Geophysical Prospecting, 69(5):913–925.

Gierse, G., J., Eisenberg-Klein, H., Trappe, H., and Pruessmann, J., 2008, CRS-PreSTM/CRS-PreSDM - Noise Reduction in Seismic Imaging: 70th Annual International Meeting, EAGE, Expanded Abstracts.

Gierse, G., J. Pruessmann, H. Trappe, H. G. Linzer, and M. Schachinger, 2015, Customized CRS regularization strategies for improved migration results: 85th Annual International Meeting, SEG, Expanded Abstracts, 3905–3909.

Glöckner, M., Dell1, S., Schwarz, B., Vanelle, C., and Gajewski, D., 2019, Velocityestimation improvements and migration/demigration using the common-reflection surface with continuing deconvolution in the time domain: Geophysics, 84(4), S229-S238

Hubral, P., 1983, Computing true-amplitude reflections in a laterally inhomogeneous earth: Geophysics, 48, 1051-1062.

Jäger, R., J. Mann, G. Höcht, and P. Hubral, 2001, Common reflection surface stack: Image and attributes: Geophysics, 66, 97–109.

Mann, J., 2001. Common-reflection-surface stack and conflicting dips. Extended Abstracts, 71th International Meeting, SEG, Expanded Abstracts, 1886-1889.

Mann, J., 2002, Extensions and applications of the common-reflection-surface stack method, Ph.D. thesis, University of Karlsruhe.

Müller, T., Jäger, R., and Höcht, G., 1998, Common reflection surface stacking method – Imaging with and unknown velocity model: Annual International Meeting, SEG, Expanded Abstract, 1764-1767.

Schuenemann, E., G. Gierse, and E. Tessmer, 2011, Reverse time migration using CRS shot gathers: 73rd Annual International Conference and Exhibition, EAGE, Extended Abstracts, cp-238.

Schleicher, J., Tygel, M., and Hubral, P., 1993, Parabolic and hyperbolic paraxial two-point traveltimes in 3D media: Geophysical Prospecting, 41, 495-513.

Spinner, M., and J. Mann, 2007, CRS-based minimum-aperture time migration: A 2D land data case study: 77th Annual International Meeting, SEG, Expanded Abstracts, 2354–2358

Tygel, M., Müller, T., Hubral, P., and Schleicher, J., 1997, Eigenwave based multiparameter traveltime expansions: 67th Annual Meeting, SEG, Expanded Abstracts, 97, 1770–1773